International Conference on Mathematics, Computational Methods & Reactor Physics (M&C 2009)
Saratoga Springs, New York, May 3-7, 2009, on CD-ROM, American Nuclear Society, LaGrange Park, IL (2009)

COUPLED ENERGY GROUP ITERATION SCHEME FOR DETERMINISTIC TRANSPORT PROBLEMS

A. M. Watson
Knolls Atomic Power Laboratory
P.O. Box 1072, Schenectady, NY 12301
watsam@kapl.gov

ABSTRACT

A coupled inner-outer iteration scheme for multigroup deterministic transport problems is introduced. Both the traditional solution method and the coupled solution method are derived, and comparisons are made using several realistic test problems. It is shown that, for a reactor problem with significant thermal upscattering, the coupled solver converged more quickly than the traditional solver. However, for a shielding problem with little upscattering, the traditional solver showed faster convergence. In addition, it is shown that as the number of energy groups increases, the coupled solver is faster, but has a larger memory footprint, than the traditional solver.

Key Words: Multigroup, Deterministic, Transport

1. INTRODUCTION

Deterministic transport codes have traditionally used the multigroup method to discretize the energy space. This approach results in a system of one-group transport problems, each of which may be solved using a variety of one-group deterministic transport solvers. These equations are only coupled in energy through a scattering matrix that represents particles moving from one energy group to another. This coupling term can be combined with an energy-dependent source term to yield an estimate of the multigroup source for each of these coupled equations; each equation can then be solved as if it is an independent problem.

In this paper, we first derive the traditional multigroup method in operator notation, and describe the traditional solution process. We then modify the derivation slightly to produce a set of equations that are not coupled in their source terms, but rather in their transport terms. This arrangement allows us to use recently developed Krylov subspace methods [1,2] to solve the system in a completely coupled form. We demonstrate that this approach is more efficient and more numerically stable than the traditional combined "inner" and "outer" iteration method. In contrast to previous work [3], we apply the coupled method to 3D problems, extend its use to different spatial methods, and use the combined flux moments and boundary face angular flux vector as the unknown.

2. THE MULTIGROUP METHOD

The multigroup transport equation with isotropic scattering and sources is defined as:

$$\underline{\Omega}\cdot\underline{\nabla}\psi_g\left(\underline{r},\underline{\Omega}\right)+\sigma_g\left(\underline{r}\right)\psi_g\left(\underline{r},\underline{\Omega}\right)=\frac{1}{4\pi}\sum_{g'=1}^{G}\sigma_{s,g'\to g}\left(\underline{r}\right)\phi_{g'}\left(\underline{r}\right)+\frac{1}{4\pi}Q_g\left(\underline{r}\right), \tag{2.1}$$

for energy group $g=1\ldots G$. We first write Eq. (2.1) in operator notation in order to make it easier to read and provide for ease of comparison between the two solution methods. The operator notation form of the multigroup transport equation is:

$$\mathbf{L}_g\psi_g=\frac{1}{4\pi}\sum_{g'=1}^{G}\mathbf{S}_{g'\to g}\phi_{g'}+q_g,\quad g=1\ldots G, \tag{2.2}$$

where ψ_g, $\phi_{g'}$, and q_g are vectors resulting from the spatial and angular discretization of the analogous continuous functions in Eq. (2.1), and where the following operators are defined:

$$\begin{aligned}&\mathbf{L}_g x_g \coloneqq \underline{\Omega}\cdot\underline{\nabla}x_g\left(\underline{r},\underline{\Omega}\right)+\sigma_g\left(\underline{r}\right)x_g\left(\underline{r},\underline{\Omega}\right),\\&\mathbf{S}_{g'\to g}x_{g'}\coloneqq\sigma_{s,g'\to g}\left(\underline{r}\right)x_{g'}\left(\underline{r}\right),\\&q_g\coloneqq\tfrac{1}{4\pi}Q_g\left(\underline{r}\right).\end{aligned}$$

2.1. Traditional Solution Method

The traditional method of solving the system described in Eq. (2.2) involves separating the within-group scattering term from the group-to-group scattering term, and progressing through the resulting linear system from group 1 (highest energy) to group *G* (lowest energy), using the latest information for computing the scattering source into each group. This is accomplished by writing Eq. (2.2) as the following, for outer iteration *k*:

$$\mathbf{L}_g\psi_g^{(k)}=\frac{1}{4\pi}\mathbf{S}_{g\to g}\phi_g^{(k)}+\frac{1}{4\pi}\sum_{g'=1}^{g-1}\mathbf{S}_{g'\to g}\phi_{g'}^{(k)}+\frac{1}{4\pi}\sum_{g'=g+1}^{G}\mathbf{S}_{g'\to g}\phi_{g'}^{(k-1)}+q_g,\quad g=1\ldots G. \tag{2.3}$$

If one combines the group-to-group scattering term with the group *g* source term, Eq. (2.3) can be written as a one-group transport equation:

$$\mathbf{L}_g\psi_g^{(k)}=\frac{1}{4\pi}\mathbf{S}_{g\to g}\phi_g^{(k)}+\tilde{q}_g^{(k,k-1)},\quad g=1\ldots G, \tag{2.4}$$

where the modified source is defined as:

$$\tilde{q}_g^{(k,k-1)}\coloneqq\frac{1}{4\pi}\sum_{g'=1}^{g-1}\mathbf{S}_{g'\to g}\phi_{g'}^{(k)}+\frac{1}{4\pi}\sum_{g'=g+1}^{G}\mathbf{S}_{g'\to g}\phi_{g'}^{(k-1)}+q_g.$$

We can write Eq. (2.4) as a linear system by moving the scattering term to the left-hand side of the equation, multiplying through by $\mathbf{L}_g^{-1}$, and integrating over all directions. This gives us:

$$\left[\mathbf{I}-\frac{1}{4\pi}\mathbf{D}\mathbf{L}_g^{-1}\mathbf{S}_{g\to g}\right]\phi_g^{(k)}=\mathbf{D}\mathbf{L}_g^{-1}\tilde{q}_g^{(k,k-1)},\quad g=1\ldots G, \tag{2.5}$$

where the operator **D** is the integral over all directions and **I** is the identity matrix. This linear system can be solved by any number of linear equation solvers, including Krylov subspace methods. However, we are primarily interested in the solution of the system of equations (the "outer" iteration), not the equation for each energy group (the "inner" iteration). The traditional solution method walks through the energy groups, from high energy to low energy, using the latest information for computing the scattering source into each group. This solution method is identical to the Gauss-Seidel iteration method [1]. Thus, we can expect the convergence rate of the outer iterations to be similar to the convergence rate of the Gauss-Seidel method applied to the scattering matrix.

2.2. Coupled Solution Method

The derivation of our coupled solution method involves simply applying the linear system solution algorithm to Eq. (2.2) without splitting the within-group scattering and group-to-group scattering terms. Thus, our system of equations is:

$$\mathbf{L}_g\psi_g=\frac{1}{4\pi}\sum_{g'=1}^{G}\mathbf{S}_{g'\to g}\phi_{g'}+q_g,\quad g=1\ldots G. \tag{2.6}$$

Using this formulation, there is no outer iteration, so the iteration index *k* is not included. We can write Eq. (2.6) as a linear system by moving the scattering term to the left-hand side of the equation, multiplying through by $\mathbf{L}_g^{-1}$, and integrating over all directions. This gives us:

$$\phi_g-\frac{1}{4\pi}\mathbf{D}\mathbf{L}_g^{-1}\sum_{g'=1}^{G}\mathbf{S}_{g'\to g}\phi_{g'}=\mathbf{D}\mathbf{L}_g^{-1}q_g,\quad g=1\ldots G, \tag{2.7}$$

where the operator **D** is the integral over all directions. This linear system contains only one level of iteration, and can be solved by any number of linear equation solvers, including Krylov subspace methods. We expect the coupled solution obtained using Eq. (2.7) to be less expensive computationally than the traditional iterative method described by Eq. (2.5) for problems where the scattering matrix is highly non-lower-triangular, such as in many reactor problems. However, for problems that are highly absorbing with little scattering, we expect the traditional iterative method to prevail.

In order to clarify the differences between the traditional and the coupled methods, we will put both equations (2.5) and (2.7) on the same basis. The equations become:

$$\left[\mathbf{I}_g - \underbrace{\frac{1}{4\pi}\mathbf{D}\mathbf{L}_g^{-1}\mathbf{S}_{g\to g}\mathbf{I}_g}_{\mathbf{1}}\right]\phi^{(k)} = \left[\underbrace{\mathbf{D}\mathbf{L}_g^{-1}\frac{1}{4\pi}\sum_{g'=1}^{g-1}\mathbf{S}_{g'\to g}\mathbf{I}_{g'}}_{\mathbf{2}}\right]\phi^{(k)} + \left[\underbrace{\mathbf{D}\mathbf{L}_g^{-1}\frac{1}{4\pi}\sum_{g'=g+1}^{G}\mathbf{S}_{g'\to g}\mathbf{I}_{g'}}_{\mathbf{3}}\right]\phi^{(k-1)} + \mathbf{D}\mathbf{L}_g^{-1}\mathbf{I}_g q, \quad g = 1\ldots G, \text{ and} \tag{2.8}$$

$$\left[\mathbf{I}_g - \underbrace{\frac{1}{4\pi}\mathbf{D}\mathbf{L}_g^{-1}\sum_{g'=1}^{G}\mathbf{S}_{g'\to g}\mathbf{I}_{g'}}_{\mathbf{4}}\right]\phi = \mathbf{D}\mathbf{L}_g^{-1}\mathbf{I}_g q, \quad g = 1\ldots G. \tag{2.9}$$

The I_g operator in these equations implies extraction of the group g flux from the global vectors. The global vectors contain the group-specific vectors as components and are denoted as $\phi^{(k)}$, ϕ, and q. One can see by comparison that the term labeled **4** in equation (2.9) is essentially the sum of terms **1**, **2**, and **3** in equation (2.8); thus, using $\mathbf{A}x = b$ as a model, they are part of the **A**-matrix in equation (2.9) as opposed to being part of the source b as in equation (2.8). This summation eliminates the need for the iteration index k in equation (2.9). This scattering term is the only difference between the traditional and coupled methods.

3. PROBLEMS AND RESULTS

In order to demonstrate the strengths and weaknesses of both the traditional multigroup iterative approach and our coupled approach, we have chosen several test problems. These problems and their results are discussed in the following sections.

3.1 PWR Pin Cell Model

In the first test problem, we model a traditional 3D PWR pin cell (dimensions and materials from Todreas & Kazimi [4]), with reflective boundaries on all sides. The model measures 12.6 mm on each side, with a pin diameter of 8.2 mm, and is extruded to a depth of 1 cm. The pin is surrounded by clad, with a thickness of 0.57 mm and a 0.08-mm gap between the pin and the clad. The pin is 2.6% enriched UO_2, the clad is zircaloy, and the gap and outer region are water. The cross sections are broadened to a temperature of 550 °F. We refer to this model as the PWR pin cell model. A diagram is shown in Figure 1. The pin, gap, and clad were modeled as 16-sided regular polygons, conserving the volume of the pin and clad. The model is meshed with 7,938 tetrahedra.

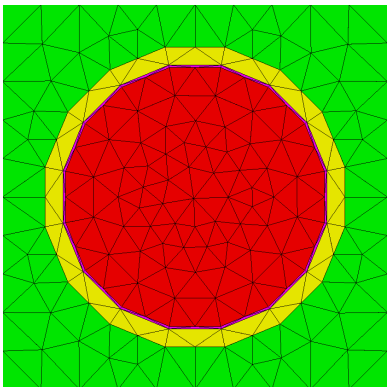

Figure 1. PWR pin cell model.

This model was run using eight different group structures, with 1, 2, 4, 8, 16, 32, 64, and 171 energy groups. The scattering matrices resulting from these group structures, averaged over the entire model, are shown in Figure 2. The colors shown represent the magnitude of the scattering cross sections, from blue (smallest) to red (largest). One can see that there is significant upscattering in the thermal regions. It is for this reason that we expect superior performance of the coupled solver for this problem.

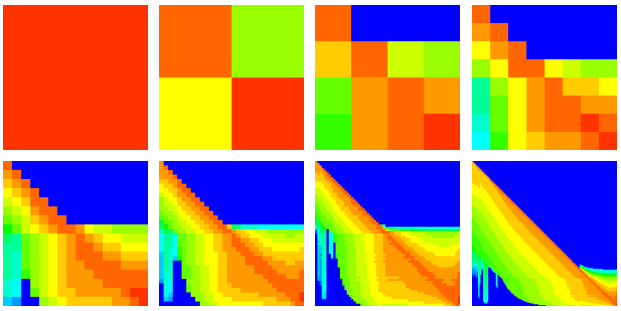

Figure 2. Scattering matrices for the PWR pin cell model for (from top left) 1, 2, 4, 8, 16, 32, 64, and 171 energy groups.

The total number of transport sweeps, computational time, and memory usage for the pin cell problem are shown in Table I. The 171-group traditional solver case exceeded the system's hard limit of 432,000 seconds for a single job. One can see that as the number of energy groups increases, the coupled solver takes a factor of six fewer sweeps than the traditional solver, which results in a factor of three speedup. Although the coupled solver needs fewer sweeps than the traditional solver, its use results in a 65% increase in memory usage. This results in a net decrease in the total computational time for the coupled solver. However, the overall advantage of this speedup is mitigated because the gain from needing fewer sweeps is spent on increased memory manipulation time. Even so, it is evident that the additional overhead required for the coupled solver over the traditional solver is offset by the decrease in computational time needed, at least up to 171 energy groups.

Table I. Results for the PWR Pin Cell Model

Groups	Traditional			Coupled		
	Sweeps	Time (s)	Memory (MB)	Sweeps	Time (s)	Memory (MB)
1	33	35.07	1	31	32.44	1
2	149	145.5	4,042	156	161.3	4,001
4	850	831.5	4,364	348	401.9	4,692
8	4,410	4,564	5,122	808	1,069	6,214
16	14,860	16,540	6,520	2,976	5,176	9,311
32	41,847	57,910	9,466	6,784	16,900	15,150
64	101,609	142,100	19,346	17,472	55,520	30,754
171	–	–	42,076	48,222	319,300	73,279

3.2 PWR Assembly Model

The second test problem consists of one-eighth of a 17×17 array assembly of the PWR pin cells. A diagram is shown in Figure 3. The figure is colored by material, where blue is water, red is fuel, grey is structure, and green is poison. We refer to this problem as the PWR Assembly Model. The problem was run with 16 energy groups and is modeled assuming one-eighth assembly symmetry, with reflective boundaries on all sides. The model is meshed with 31,076 tetrahedra.

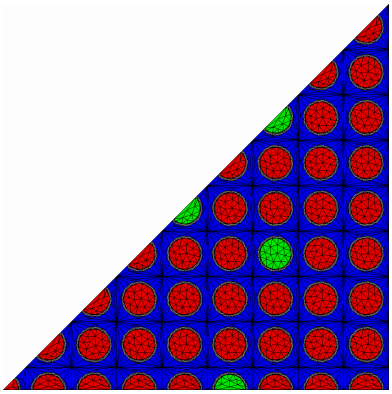

Figure 3. PWR assembly model.

The fast and thermal flux solutions of this model are shown in Figure 4. The number of sweeps, total computational time, and memory footprint of both solvers, as well as the relative differences in these metrics are shown in Table II. The traditional solver needed a total of 12,843 sweeps, took 58,830 seconds, and used 22,476 MB of memory to solve the problem. The

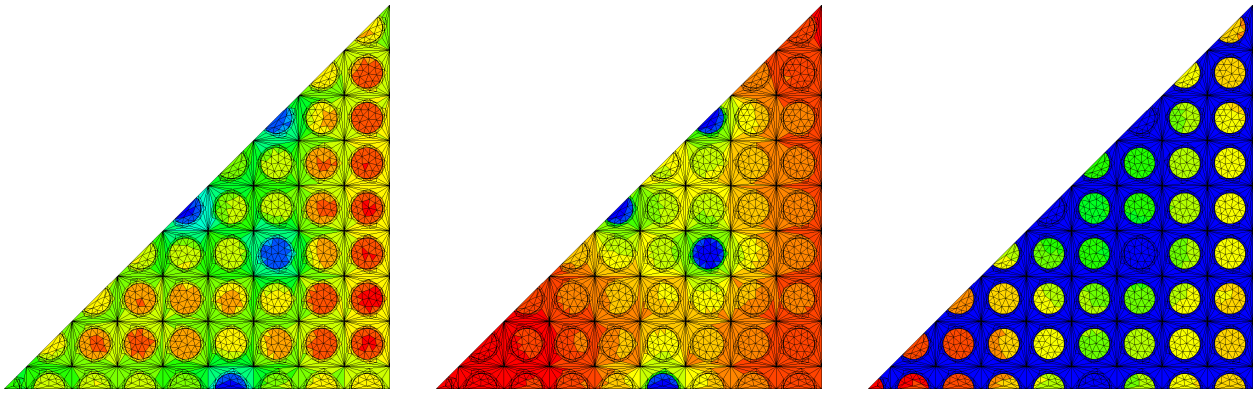

(a) (b) (c)

Figure 4. PWR assembly model results: (a) fast flux, (b) thermal flux, and (c) relative power density.

coupled solver needed a total of 2,464 sweeps, took 17,190 seconds, and used 37,513 MB of memory to solve the problem. Therefore, the coupled solver needed a factor of five fewer sweeps, had a factor of three speedup, and used 67% more memory than the traditional solver. These results are consistent with our expectations developed from the pin cell model.

Table II. Results for the PWR assembly model.

Metric	Traditional	Coupled	C/T–1
Sweeps	12,843	2,464	-80.8%
Time (s)	58,830	17,190	-70.8%
Memory (MB)	22,476	37,513	+66.9%

3.3 Shippingport Shielding Model

The third test problem is a model of the Shippingport reactor containment and shield tank. This problem was chosen to compare the two methods on a problem with little upscattering. A diagram of the model is shown in Figure 5. This problem was run with 15 neutron energy groups and 1 gamma group, using coupled neutron-gamma cross sections. The outside of the containment has a vacuum boundary condition, with reflective boundaries on the other two sides. The model is meshed with 131,792 tetrahedra.

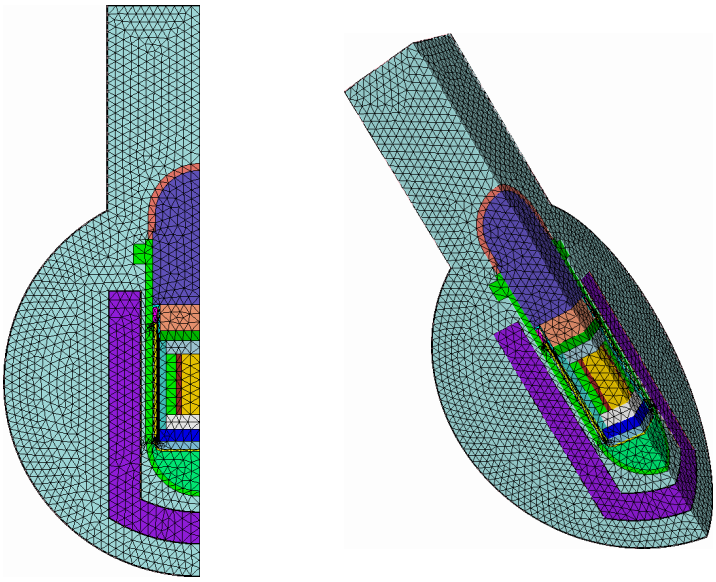

Figure 5. Shippingport reactor containment and shield tank model.

The scattering matrix resulting from the group structure used in this model—15 neutron groups (14 fast and 1 thermal) and 1 gamma group—averaged over the entire model is shown in Figure 6. The colors shown represent the magnitude of the scattering cross sections, from blue (smallest) to red (largest). One can see that there is no upscattering in this matrix. It is for this reason that we expect superior performance of the traditional solver for this problem.

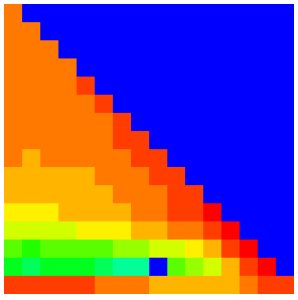

Figure 6. Scattering matrix for the Shippingport model for 15 neutron groups (14 fast and 1 thermal) and 1 gamma group.

The total relative dose solution of this model is shown in Figure 7. The number of sweeps, total computational time, and memory footprint of both solvers, as well as the relative differences in these metrics are shown in Table III. The traditional solver needed a total of 777 sweeps, took 16,080 seconds, and used 108,087 MB of memory to solve the problem. The coupled solver needed a total of 2,976 sweeps, took 67,270 seconds, and used 146,912 MB of memory to solve

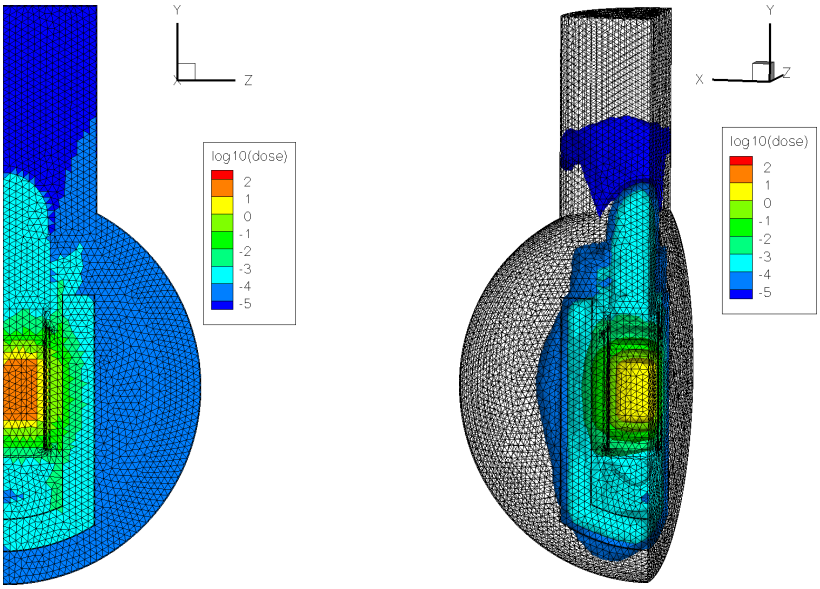

Figure 7. Shippingport total relative dose solution.

Table III. Results for the Shippingport model.

Metric	Traditional	Coupled	C/T–1
Sweeps	777	2,976	+283%
Time (s)	16,080	67,270	+318%
Memory (MB)	108,087	146,912	+35.9%

the problem. Therefore, the traditional solver needed a factor of four fewer sweeps, had a factor of four speedup, and used 26% less memory than the coupled solver. These results are consistent with our expectations for a problem with little upscattering.

4. CONCLUSIONS

We have shown several test problems in this paper comparing the traditional and coupled solvers. These problems are representative of typical reactor core and shielding problems. For the reactor problem with significant thermal upscattering, we demonstrated that the coupled solver converged faster than the traditional solver, by a factor of three, for a 67% increase in memory usage. However, for the shielding problem with little upscattering, the traditional solver showed faster convergence by a factor of four. In addition, we have demonstrated using a pin cell model that as the number of energy groups increases, the coupled solver is faster by about a factor of three with a 65% larger memory footprint than the traditional solver.

ACKNOWLEDGEMENTS

The author would like to thank Michael Bassett and the shielding group at KAPL for building the Shippingport model, and for their assistance in creating cross sections for the model.

REFERENCES

1. J.S. Warsa, T.A. Wareing, and J.E. Morel, "Krylov Iterative Methods Applied to Multidimensional S_N Calculations in the Presence of Material Discontinuities," *Proc. M&C 2003*, Gatlinburg, Tennessee (2003).
2. J.S. Warsa, T.A. Wareing, J.E. Morel, J.M. McGhee, R.B. Lehoucq, "Krylov Subspace Iterations for the Calculation of k-Eigenvalues with S_N Transport Codes," *Proc. M&C 2003*. Gatlinburg, Tennessee (2003).
3. B.W. Patton and J.P. Holloway, "Application of preconditioned GMRES to the numerical Solution of the Neutron Transport Equation," *Ann. Nucl. Energy*, **29**:109–136 (2002).
4. N.E. Todreas and M.S. Kazimi, *Nuclear Systems I: Thermal Hydraulic Fundamentals*, Taylor & Francis (1993).